Origin of the scaling law in human mobility: Hierarchy of traffic systems

Xiao-Pu Han,[1] Qiang Hao,[1] Bing-Hong Wang,[1] and Tao Zhou[1,2,*]

[1]*Department of Modern Physics, University of Science and Technology of China, Hefei 230026, People's Republic of China*

[2]*Web Sciences Center, University of Electronic Science and Technology of China, Chengdu 610051, People's Republic of China*

(Received 5 June 2010; revised manuscript received 18 January 2011; published 30 March 2011)

Uncovering the mechanism leading to the scaling law in human trajectories is of fundamental importance in understanding many spatiotemporal phenomena. We propose a hierarchical geographical model to mimic the real traffic system, upon which a random walker will generate a power-law-like travel displacement distribution with tunable exponent, and display a scaling behavior in the probability density of having traveled a certain distance at a certain time. The simulation results, analytical results, and empirical observations reported in D. Brockmann *et al.* [Nature (London) **439**, 462 (2006)] agree very well with each other.

DOI: 10.1103/PhysRevE.83.036117 PACS number(s): 89.75.Fb, 05.40.Fb, 89.75.Da

I. INTRODUCTION

Studies on the non-Poisson statistics of human behaviors have recently attracted much attention [1–3]. Besides the interevent or waiting time distribution, the spatial movements of humans also exhibit non-Poisson statistics. Brockmann *et al.* [4] investigated the bank note dispersal as a proxy for human movements, and revealed a power-law distribution of human travel displacements. Gonzalez *et al.* [5] studied the human travel patterns by measuring the distance of mobile phone users' movements in different stations, and observed a similar scaling law. From the GPS data, Jiang *et al.* [6] observed a Lévy flight behavior of human mobility in a large-scale street network. The mobility patterns of many animals also show power-law-like displacement distributions [7]. Some interpretations, such as optimal search strategy [8], olfactory-driven foraging [9], and deterministic walks [10], have already been raised, however, they are based on the prey processes and thus cannot be used to explain the observed scaling law in human trajectories. We propose a model to mimic the human travel pattern, where the hierarchical organization of human traffic systems is taken into account. Agreeing very well with the empirical observations, our model can reproduce the power-law displacement distributions, as well as the scaling behavior in probability density of having traveled a certain distance at a certain time.

II. MODEL

In human traffic systems, a district (e.g., a province or a state) usually has a core city, like its capital, around which there are several big cities as the secondary centers (e.g., municipalities), each of which is rounded by some counties; and towns and villages surround each county. A hierarchical traffic system is built accordingly. Imagine people traveling from a town a subordinating to the central city A, to another town b subordinating to the central city B. There is usually no direct way connecting a and b, and the typical route is $a \to A \to B \to b$, which may be much longer than the geographical distance between a and b. Such a hierarchical organization and the resulting scale invariance in road networks have already been demonstrated [11].

In our model, we call all the units *cities*, which are organized in N layers. Denote K the number of first-layer cities, and M the ratio of the next-layer cities to the current-layer cities. KM^{N-1} cities, including K first-layer cities, $K(M-1)$ second-layer cities, ..., $KM^{n-2}(M-1)$ nth-layer ($n \geqslant 2$) cities, ..., and $KM^{N-2}(M-1)$ Nth-layer cities, are randomly distributed in an $S \times S$ continuous square. Each of the nth-layer ($1 < n \leqslant N$) cities is connected to its nearest higher-layer city, and two nth-layer cities are connected if they are connected to the same higher-layer city. The first layer corresponds to the top layer, in which the cities are fully connected with each other. A system with $N = 3$, $M = 5$, and $K = 2$ is illustrated in Fig. 1, where 50 cities (2 first-layer cities, 8 second-layer cities, and 40 third-layer cities) are distributed on a square. Each of the third-layer cities is connected to its nearest second-layer city or first-layer city, and each of the second-layer cities is connected to its nearest first-layer city, and two first-layer (the top layer) cities are also connected. Two cities in the same layer are connected if they connect to the same higher-layer city. For example, all the second-layer cities that connect to the first-layer city B are fully connected to each other, as shown in Fig. 1(c), as well as the third-layer cities shown in Fig. 1(b). Notice that a third-layer city is allowed to connect directly to a first-layer city if this first-layer city is the third-layer city's nearest higher-layer city. For instance, there are five third-layer cities connecting to the first-layer city A in Fig. 1(a), and thus the organization is not exactly hierarchical. Using this algorithm, we can create a quasihierarchical geographical system on the square two-dimensional square field, which is close to the organization in real-world traffic systems.

We consider the simplest case where a random walker is consequently jumping from the current occupied city to a random neighbor (two cities are said to be neighboring if they are connected) at each time step. The displacement L of the walker in one step is defined as the corresponding geometric distance. Figure 1(a) shows a typical trajectory of a walker moving from a lower-layer city to a higher-layer city in eight consecutive time steps, in which the length of each arrow corresponds to the displacement of the movement in each time step. In the real world, a central city is generally

*zhutou@ustc.edu

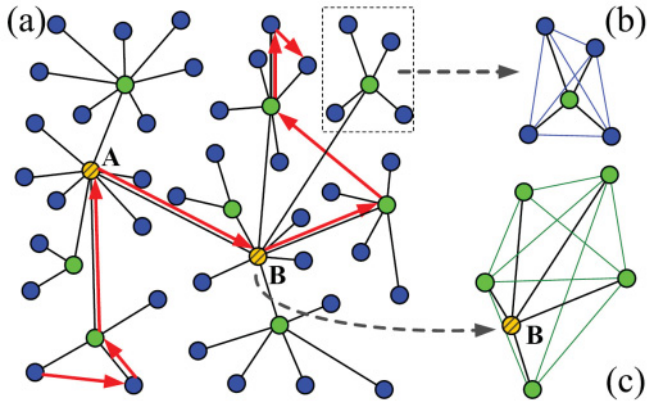

FIG. 1. (Color online) (a) Illustration of an eight-step travel in a three-layer system ($N = 3$, $M = 5$ and $K = 2$), where orange (with oblique lines), green (light gray), and blue (dark gray) nodes respectively denote the first-, second-, and third-layer cities. For clarity, we do not plot the connections between cities in the same layer, except the one between the two first-layer cities, A and B. (b) All the connections in the domain of a second-layer city and its surrounded third-layer cities. (c) All the connections in the domain of the first-layer city B and its surrounded second-layer cities.

more attractive than a small town, which is represented by a layer-dependent weight, $w_n = r^{N-n}$, where n denotes the layer and $r \geqslant 1$ is a free parameter. The probability that the walker will move to a neighboring city is proportional to its weight, namely, $\Pi_i = w_i / \sum w_j$, where Π_i is the probability that the walker moves to the ith neighboring city, and $\sum w_j$ is the total weight of all the neighboring cities. Clearly, a larger r indicates higher heterogeneity. The essential physics of this model is a weighted random-walk process [12] in a geographical network where edges are of different geometric lengths. For a random walker in a connected symmetry (undirected) network, in the long time limit, each edge has the same chance to be visited (this proposition holds even for a very heterogeneous network, since for an arbitrary node, the number of times being visited is proportional to its degree while the probability that a specific adjacent edge of this node is consecutively visited is inversely proportional to the degree. Details can be found in Ref. [13]). Therefore when $r = 1$, the displacement distribution of a random walker is equivalent to the distribution of edges' geometric lengths.

III. SIMULATION

Figure 2(a) shows the trajectory for $r = 2.0$ in a five-layer system, where the occurrences of long-range travels are clearly observed. As shown in Fig. 2(b), the displacement distribution is heavy tailed and can be well fitted by a power law with an exponential cutoff, as $P(L) = cL^{-\beta}e^{-\lambda L}$. The fitting parameters, β and λ, are obtained by using the *maximum likelihood estimation* [14]. When r increases from 1.0 to 2.0, the power-law exponent, β, monotonously decreases from 3.11 to 1.63, covering the range of empirical observations [4–6]. As shown in Fig. 3, smaller M makes the travels between lower-layer and higher-layer cities more frequent, and thus enhances the long displacements. This effect is more

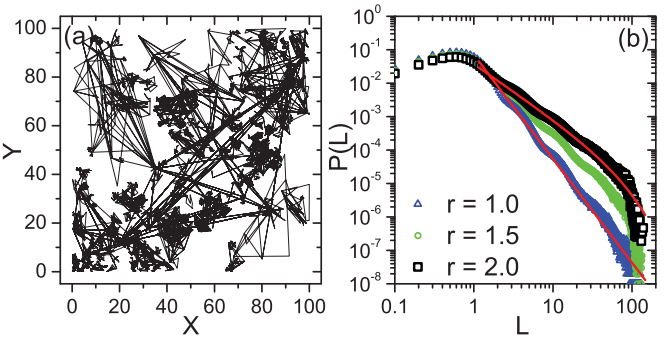

FIG. 2. (Color online) (a) The trajectory of a walker in 5000 consecutive steps. (b) Displacement distribution $P(L)$, averaged by 1000 independent runs, each of which lasts 10^5 time steps. The parameters are $N = 5$, $M = 9$, $K = 9$, and $S = 100$. In (a), $r = 2.0$. The red (light gray) solid lines denote the fitting functions, $f(L) = 0.070L^{-3.11}e^{-0.0L}$ for $r = 1.0$, and $f(L) = 0.038L^{-1.63}e^{-0.015L}$ for $r = 2.0$.

remarkable when $r > 1$, because in the case of a larger r, the travels to higher-layer cities are more frequent. As shown in Fig. 4, in contrast to the observable effects of r and M, the displacement distribution $P(L)$ is not sensitive to the parameters N and K.

IV. ANALYSIS

Let us consider the situation that m cities are randomly distributed in an $S \times S$ square. If the geometric distance of two cities in the square is D, to eliminate the effect of square size we define the rate of distance as $d = D/S$. Ignoring the boundary effects of the square (i.e., in the case of $d \ll 1$), the normalized probability density of the distance from a city to its nearest city (these two cities are not necessarily connected) is

$$\Phi(d) \approx (m-1) \times 2\pi d(1-\pi d^2)^{m-2}, \qquad (1)$$

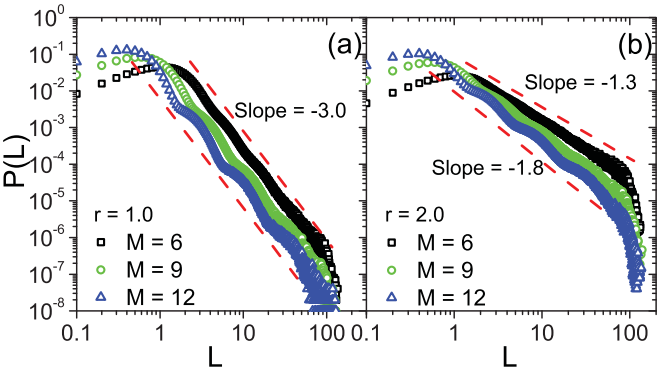

FIG. 3. (Color online) Displacement distribution $P(L)$ for different M, obtained by 1000 independent runs, each of which lasts 10^5 time steps. Panels (a) and (b) respectively correspond to the cases of $r = 1.0$ and $r = 2.0$. The parameters are $N = 5$, $K = 9$, and $S = 100$. The red (light gray) dashed lines denote the power laws with the corresponding exponents.

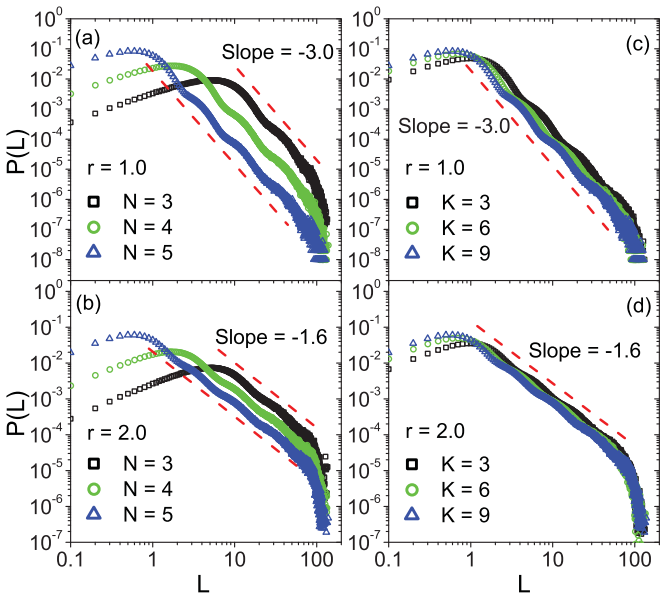

FIG. 4. (Color online) Displacement distribution $P(L)$ for different N with (a) $r = 1.0$ and (b) $r = 2.0$, and for different K with (c) $r = 1.0$ and (d) $r = 2.0$. Other parameters are $M = 9$ and $S = 100$. All the data points are averaged by 1000 independent runs, each of which lasts 10^5 time steps. The red (light gray) dashed lines denote the power laws with the corresponding exponents.

where $(m-1)$ is the normalization factor of the distribution. From $\partial P(d)/\partial d|_{d=d_*} = 0$, the maximum likelihood distance is $d_* = [(2m-3)\pi]^{-1/2}$, corresponding to

$$\Phi(d_*) = (m-1)\sqrt{\frac{4\pi}{2m-3}}\left(1-\frac{1}{2m-3}\right)^{m-2}. \quad (2)$$

For a very large m, $d_* \approx (2\pi m)^{-1/2}$ and $(1-\pi d_*^2)^{1/\pi d_*^2} \approx e$, therefore

$$\Phi(d_*) \approx d_*^{-1} e^{-1/2}. \quad (3)$$

Approximately, all the $(n+1)$th-layer cities connected with a higher-layer (i.e., from first-layer to nth-layer) city are distributed inside a circle, and thus the length of an edge between an $(n+1)$th-layer city to its nearest higher-layer city can be roughly estimated as the average distance from a random point in a unit circle to its center (since we only care about the relative ratio, the radius of the circle plays no role), namely $d' = \int\int_{x^2+y^2\leqslant 1}\sqrt{x^2+y^2}dxdy = 0.667$. Analogously, the length of an edge between two $(n+1)$th-layer cities can be estimated as $d'' = \int\int\int\int_{x_1^2+y_1^2\leqslant 1, x_2^2+y_2^2\leqslant 1}\sqrt{(x_1-x_2)^2+(y_1-y_2)^2}dx_1dy_1dx_2dy_2 = 0.905$. That is to say, $d'' = \sigma d'$ where $\sigma \approx 1.36$ is a constant. The total number of the cities from the first layer to the nth layer is KM^{n-1}, thus the corresponding maximum likelihood length from an $(n+1)$th-layer city to its nearest higher-layer city is $d_{*,n+1} = (2\pi KM^{n-1})^{-1/2}$ (in this case, $m = KM^{n-1}$). We therefore have

$$-\frac{\ln(M^{n-1})}{\ln r} = \frac{\ln\left(2\pi K d_{*,n+1}^2\right)}{\ln r}, \quad (4)$$

$$r^{N-n} = r^{N-1}\left(2\pi K d_{*,n+1}^2\right)^{\ln_M r}. \quad (5)$$

Denote by u_n the probability that the walker stays in the nth layer during the walking process, the equilibrium condition reads

$$(q_+ + q_-)u_n = q_+u_{n-1} + q_-u_{n+1}, \quad 1 < n < N, \quad (6)$$

where q_+ and q_- denote the probability that the walker moves to the next lower and higher layer, respectively. Since there are $KM^{n-1}(M-1)$ $(n+1)$th-layer cities and in total KM^{n-1} cities from first layer to nth layer, an nth-layer city averagely connects to $(M-1)$ $(n+1)$th-layer cities. And there are $KM^{n-3}(M-1)$ $(n-1)$th-layer cities among KM^{n-2} cities from first layer to $(n-1)$th layer, an nth-layer city averagely connects to a $\frac{M-1}{M}$ $(n-1)$th-layer city. Therefore

$$q_+ \approx \frac{M-1}{(M-1)+(M-2)r+(1-\frac{1}{M})r^2},$$
$$q_- \approx \frac{(1-\frac{1}{M})r^2}{(M-1)+(M-2)r+(1-\frac{1}{M})r^2}. \quad (7)$$

Considering the self-similar structure, we have

$$u_n/u_{n+1} \approx u_{n-1}/u_n, \quad 1 < n < N. \quad (8)$$

Combining Eqs. (6) and (8), the ratio is $u_n/u_{n+1} = q_-/q_+ \approx r^2/M$, namely $u_n \sim r^{-2n}$.

Denote by v_{n+1} the probability that the walker moves along edges connecting $(n+1)$th- and nth-layer cities during the walking process, then according to Eq. (6), $v_{n+1} = q_-u_{n+1} + q_+u_n = 2q_+u_n$. Then the occurrence probability is

$$P(d_{*,n+1}) \sim \Phi(d_{*,n+1})v_{n+1} \sim d_{*,n+1}^{-1}e^{-1/2}u_n. \quad (9)$$

From Eqs. (5), (9), and (10), we obtain

$$P(d_*) \sim d_*^{-(3-4\ln_M r)}. \quad (10)$$

Denote by w_{n+1} the probability that the walker moves along edges connecting two $(n+1)$th-layer cities, and by $l_{*,n+1}$ the maximum likelihood length of such edges corresponding to $d_{*,n+1}$, namely $l_{*,n+1} = \sigma d_{*,n+1}$, then $w_{n+1} = (1-q_+-q_-)u_{n+1} \sim \frac{(M-2)r}{M-1}q_+\frac{Mu_n}{r^2} \sim q_+u_n \sim v_{n+1}$. Analogously, the occurrence probability is

$$P(l_*) \sim l_*^{-(3-4\ln_M r)}. \quad (11)$$

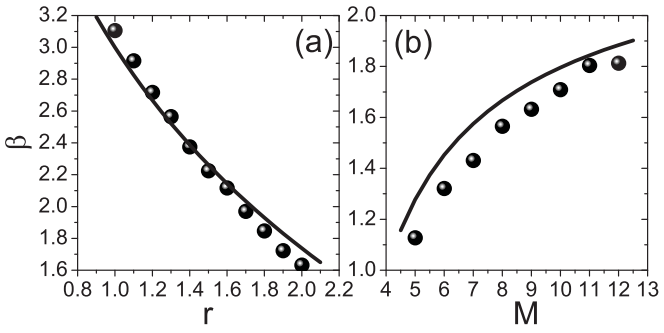

FIG. 5. (a) β vs r when $M = 9$, and (b) β vs M when $r = 2.0$. Circles are simulation results and solid lines denote the analytical solution $\beta = 3 - 4\ln_M r$. Other parameters are $N = 5$, $S = 100$, and $K = 9$.

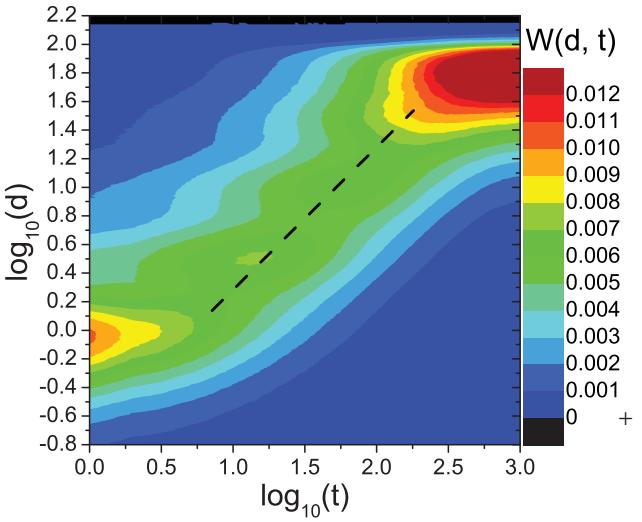

FIG. 6. (Color online) The probability $W(d,t)$ of having traveled a distance d at time t. The parameters are $N = 5, M = 9, K = 9, S = 100$, and $r = 2.0$. This plot is obtained by averaging 1000 independent runs, each of which lasts 10^4 time steps. The black dashed line, as a guide of eyes, is of slope 1.

According to Eqs. (10) and (11), we infer that the displacement distribution of the whole walking process also obeys the power-law distribution $P(L) \sim L^{-\beta}$ with the exponent $\beta = 3 - 4\ln_M r$.

As shown in Fig. 5, the approximate analysis agrees well with the simulation results. Notice that, when r is large, the analytical solution of β is slightly larger than the simulation result. As shown in Eqs. (10) and (11), our analysis only takes into account the contributions of movements within a layer or connecting two neighboring layers. However, the walker can directly jump from an nth-layer city to an $(n-2)$th-layer city, or even a higher layer. Each of this kind of movement is usually associated with one high-layer city and corresponding to a longer displacement. Since the weight of an nth-layer city is $w_n = r^{N-n}$, for a high-layer city (i.e., small n), larger r corresponds to relatively larger weight as well as the higher occurrence probability of the above-mentioned movements. This is the reason why the exponent β of simulation is slightly smaller than the analytical solution when r is large. There are slight oscillations on $P(L)$ when M is large, which is caused by the discontinuation of the typical sizes of different layers in the strictly hierarchical structure. The real-world traffic system is not so strictly hierarchical, and thus the oscillations are not expected.

Finally, we check whether our model can reproduce the spatiotemporal statistics of real human mobility. Providing the trajectory of a random walker, one can obtain the probability $W(d,t)$ of having traveled a distance d at time t. Here $d(t)$ is the distance between the walker's locations at time t_0 and $t_0 + t$. If the trajectory consists of $(T+1)$ discrete locations at time steps $0,1,\ldots,T$, then for a given t, there are $(T-t+1)$ distances for the location pairs at time steps $(0,t),(1,t+1),\ldots,(T-t,T)$. All the distances d for different t constitute the distribution $W(d,t)$. The same technique has been adopted in preparing Fig. 2(a) in Ref. [4]; please see details there. As shown in Fig. 6, a scaling behavior $d(t) \sim t^{\alpha}$ with $\alpha \approx 1.0$ is clearly observed, which agrees well with the empirical result, $\alpha \approx 0.95$, reported in Ref. [4]. Notice that there are two isolated regions, respectively, in the left bottom and right top of Fig. 6. The left-bottom region corresponds to the traveled distance in a few steps, while the right-top region comes from the finite-size effect, namely the boundary size limits the growth of d. In accordance with our results, the values of W in the left-bottom and right-top regions of Fig. 2(a) in [4] are also remarkably higher than other regions near the blue line. Similar scaling behavior can also be observed for $r = 1.0$, however, the exponent, $\alpha \approx 0.5$, is far less than the empirical value. In addition, providing the travel displacement distribution, this scaling behavior with $\alpha \approx 1.0$ cannot be reproduced by a Lévy flight [4].

V. CONCLUSIONS AND DISCUSSIONS

Uncovering the human traveling pattern is of fundamental importance in the understanding of various spatiotemporal phenomena [4–6], and may find applications in the design of traffic systems [15], the control of human infectious disease [16] and mobile virus spreading [17], the military service planning [18], the prediction of human mobility [19], and so on. Although empirical results about the scaling law of long-range human travels have been reported for years, it lacks the understanding of the underlying mechanism. Inspired by the observed hierarchical organization of disparate networks [20], our model describes a random walk process in hierarchical Euclidean networks. Although the assumption of random walking process is the simplest one in the description of human travels, our model can well reproduce the spatiotemporal statistics of mobility and reveal the spatial effects of hierarchical organization, implying the human traveling behaviors are strongly affected by the geographical structure of traffic systems. Our model not only provides a possible origin for the emergence of scaling law in human mobility patterns, but also contributes to the understanding of the correlations and interactions between human activities and the organization of social environment.

ACKNOWLEDGMENTS

We thank Changsong Zhou and Aaron Clauset for valuable suggestions. This work was supported by NNSFC (Grants No. 10635040, No. 10975126, No. 70871082, and No. 70971089).

[1] A.-L. Barabási, Nature (London) **435**, 207 (2005).
[2] A. Vázquez, J. G. Oliveira, Z. Dezsö, K. I. Goh, I. Kondor, and A.-L. Barabási, Phys. Rev. E **73**, 036127 (2006).
[3] T. Zhou, X.-P. Han, and B.-H. Wang, in *Science Matters: Humanities as Complex Systems*, edited by M. Burguete and L. Lam (World Scientific, Singapore, 2008), pp. 207–233.

[4] D. Brockmann, L. Hufnagel, and T. Geisel, Nature (London) **439**, 462 (2006).

[5] M. C. González, C. A. Hidalgo, and A.-L. Barabási, Nature (London) **453**, 779 (2008).

[6] B. Jiang, J. Yin, and S. Zhao, Phys. Rev. E **80**, 021136 (2009).

[7] F. Bartumeus, F. Peters, S. Pueyo, C. Marrasé, and J. Catalan, Proc. Natl. Acad. Sci. USA **100**, 12771 (2003); G. Ramos-Fernández, J. L. Mateos, O. Miramontes, G. Cocho, H. Larralde, and B. Ayala Orozco, Behav. Ecol. Sociobiol. **55**, 223 (2004); D. W. Sims, E. J. Southall, N. E. Humphries, G. C. Hays, C. J. A. Bradshaw, J. W. Pitchford, A. James, M. Z. Ahmed, A. S. Brierley, M. A. Hindell, D. Morritt., M. K. Musyl, D. Righton, E. L. C. Shepard, V. J. Wearmouth, R. P. Wilson, M. J. Witt, and J. D. Metcalfe, Nature (London) **451**, 1098 (2008).

[8] G. M. Viswanathan, S. V. Buldyrev, S. Havlin, M. G. E. da Luzk, E. P. Raposok, and H. E. Stanley, Nature (London) **401**, 911 (1999); F. Bartumeus, J. Catalan, U. L. Fulco, M. L. Lyra, and G. M. Viswanathan, Phys. Rev. Lett. **88**, 097901 (2002).

[9] A. M. Reynolds, Phys. Rev. E **72**, 041928 (2005).

[10] M. C. Santos, D. Boyer, O. Miramontes, G. M. Viswanathan, E. P. Raposo, J. L. Mateos, and M. G. E. da Luz, Phys. Rev. E **75**, 061114 (2007).

[11] V. Kalapala, V. Sanwalani, A. Clauset, and C. Moore, Phys. Rev. E **73**, 026130 (2006).

[12] Q. Ou, Y.-D. Jin, T. Zhou, B.-H. Wang, and B.-Q. Yin, Phys. Rev. E **75**, 021102 (2007).

[13] L. Lovász, in *Combinatorics, Paul Erdös is Eighty*, edited by D. Miklós, V. T. Sós, and T. Szönyi (Janos Bolyai Mathematical Society, Budapest, 1996), Vol. 2, pp. 353–398.

[14] A. Clauset, C. R. Shalizi, and M. E. J. Newman, SIAM Rev. **51**, 661 (2009).

[15] M. Barthélemy and A. Flammini, J. Stat. Mech. L07002 (2006).

[16] L. Hufnage, D. Brockmann, and T. Geisel, Proc. Natl. Acad. Sci. USA **101**, 15124 (2004); D. Balcan, H. Hu, B. Goncalves, P. Bajardi, C. Poletto, J. J. Ramasco, D. Paolotti, N. Perra, M. Tizzoni, W. V. den Broeck, V. Colizza, and A. Vespignani, BMC Med. **7**, 45 (2009).

[17] P. Wang, M. C. González, C. A. Hidalgo, and A.-L. Barabási, Science **324**, 1071 (2009).

[18] M. Zhao, L. Mason, and W. Y. Wang, in *Empirical Study on Human Mobility for Mobile Wireless Networks*, Proceedings of the Military Commun. Conference 2008 (IEEE Press, San Diego, 2008), pp. 1–7.

[19] C. Song, Z. Qu, N. Blumm, and A.-L. Barabási, Science **327**, 1018 (2010).

[20] M. Sales-Pardo, R. Guimerà, A. A. Moreira, and L. A. N. Amaral, Proc. Natl. Acad. Sci. USA. **104**, 15224 (2007); A. Clauset, C. Moore, and M. E. J. Newman, Nature (London) **453**, 98 (2008).